

Inelastic Alpha-Particle Excitation in the Even Tin Isotopes

N. BARON, R. F. LEONARD, JOHN L. NEED, AND W. M. STEWART

Lewis Research Center, National Aeronautics and Space Administration, Cleveland, Ohio

AND

V. A. MADSEN*

Oregon State University, Corvallis, Oregon

(Received 7 February 1966)

Angular distributions were measured for elastic and inelastic alpha-particle scattering by isotopically enriched targets of ^{116}Sn , ^{118}Sn , ^{120}Sn , and ^{122}Sn using the 40-MeV alpha beam of the NASA 60-inch cyclotron. Two states of energies close to 1.2 and 2.4 MeV were the only strong excitations observed. The inelastically scattered groups of alpha particles were analyzed using a distorted-wave Born approximation (DWBA) and the nuclear vibrational model. The results of these calculations are in good agreement with the known spins and parities: 2^+ for the first excited state and 3^- for the second. DWBA calculations were also carried out for the 2^+ excitations using eigenfunctions of the pairing plus $Q \cdot Q$ potentials. The calculated cross sections show a tendency to decrease with increasing neutron number. The experimental trend is qualitatively similar but much less regular. The absolute cross sections calculated using only cloud configurations are short of experimental values by about a factor of 4 when the Gammel-Thaler 40-MeV proton-alpha interaction is used. The relation of this discrepancy to the contribution from extracloud configurations is discussed.

INTRODUCTION

IN studies of nuclear inelastic scattering to collective states using the distorted-wave Born approximation (DWBA), close agreement with experiment has been obtained with only the interaction strength as a free parameter, since the optical parameters for the distorted waves were obtained from elastic scattering fits. The interaction strength is not really free, since in the nuclear-vibrational model it is proportional to the deformation parameter β , which may be obtained from other reactions. In the use of a particle model for the nuclear states, the strength is again not a free parameter, since it is related to the free nucleon-projectile interaction strength. The relation need not be simple, however, because of the presence of other nucleons and because the interaction is treated in first order in the DWBA and exactly in free collisions. In fact, it may be optimistic to expect a simple local interaction to be capable of representing the collisions that produce the nuclear excitation. Empirical studies are important in order to obtain further information on the interaction.

In a recent calculation¹ of the absolute cross section for excitation of the first excited state of ^{68}Ni by 40-MeV alpha particles, satisfactory agreement with experiment was obtained using a phenomenological potential obtained by Gammel and Thaler² by analysis of data for elastic scattering of protons from alpha particles. However, in addition to the uncertainties discussed above, the strength of the phenomenological free-particle potentials decreases with increasing energy, so it is not clear even what free-particle strength is appropriate. The present experimental study was undertaken both

to obtain further information about the interaction strength and to make comparisons of the ratios of absolute differential cross sections from one isotope to another with the prediction of the distorted-wave calculations. The particle-model calculations are made under the reasonable assumption that the same alpha-particle-nucleon interaction strength is appropriate for all the isotopes, so the calculated cross-section ratios are independent of interaction strength. The distorted-wave calculations of the relative cross sections as a function of neutron number provide a test of the systematics of the nuclear wave functions.

EXPERIMENTAL RESULTS

Angular distributions were measured for elastic and inelastic scattering of alpha particles by isotopically enriched targets of ^{116}Sn , ^{118}Sn , ^{120}Sn , and ^{122}Sn using the 40-MeV alpha particle beam of the NASA 60-inch cyclotron. The scattering system, pictured in Fig. 1, included magnetic analysis of the incident beam and particle detection by lithium-drifted silicon semiconductor counters. The over-all energy resolution of the experiment was held between 80 and 120 keV. Cross sections were obtained for elastic scattering ($20^\circ < \theta_{c.m.} < 150^\circ$) and for the excitation of two strongly excited states ($20^\circ < \theta_{c.m.} < 90^\circ$) in each of four even tin isotopes. No other strong excitations were observed. A typical energy spectrum is pictured in Fig. 2. The diffraction peaks in the angular distribution are about 10° apart, necessitating the collection of data every 2° . The experimental angular resolution was 1° . Details of the experimental procedure and tabular data on the cross sections are given elsewhere.³ Experimental angular distributions are shown in Figs. 3 to 6.

* Supported in part by a grant from the Oregon State University General Research Fund and in part by the U. S. Atomic Energy Commission.

¹ V. A. Madsen and W. Tobocman, *Phys. Rev.* **139**, B864 (1965).

² J. L. Gammel and R. M. Thaler, *Phys. Rev.* **109**, 2041 (1958).

³ N. Baron, R. F. Leonard, J. L. Need, and W. M. Stewart, National Aeronautics and Space Administration Report No. NASA TN D-3067, 1965 (unpublished).

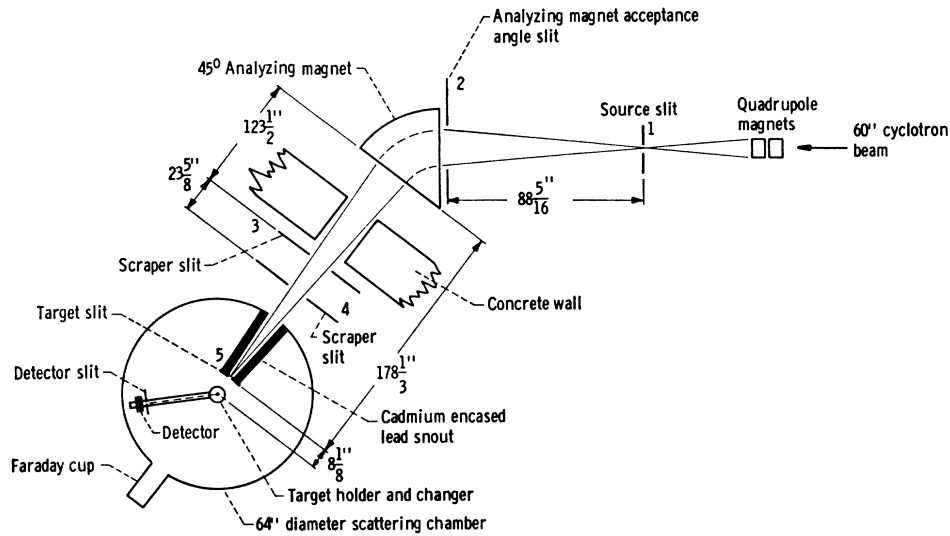


FIG. 1. Schematic diagram of scattering system.

The excitation energies of the states were determined using elastic scattering over a range of angles, with correction for target thickness, to calibrate the total electronic system. The principal source of error is in the determination of peak locations and amounts to ± 14 keV. The energies so determined are listed in Table I. They are in good agreement with previously determined values for the 2^+ and 3^- levels in the tin isotopes.

ANALYSIS OF ELASTIC SCATTERING DATA

For each of the four elastic angular distributions, an optical model analysis was performed.⁴ The assumed optical potential is written as

$$U(r) = V_C(r) - (V + iW)(1 + e^{-(r-r_0 A^{1/3})/a})^{-1}, \quad (1)$$

where $V_C(r)$ is the Coulomb electrostatic potential, V

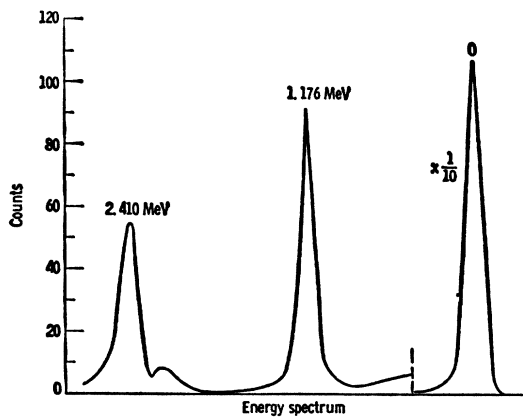


FIG. 2. Typical energy spectrum.

⁴ M. A. Melkanoff, J. S. Nodvik, D. S. Saxon, and D. G. Cantor, University of California Publication in Automatic Computation 1, 1961 (unpublished).

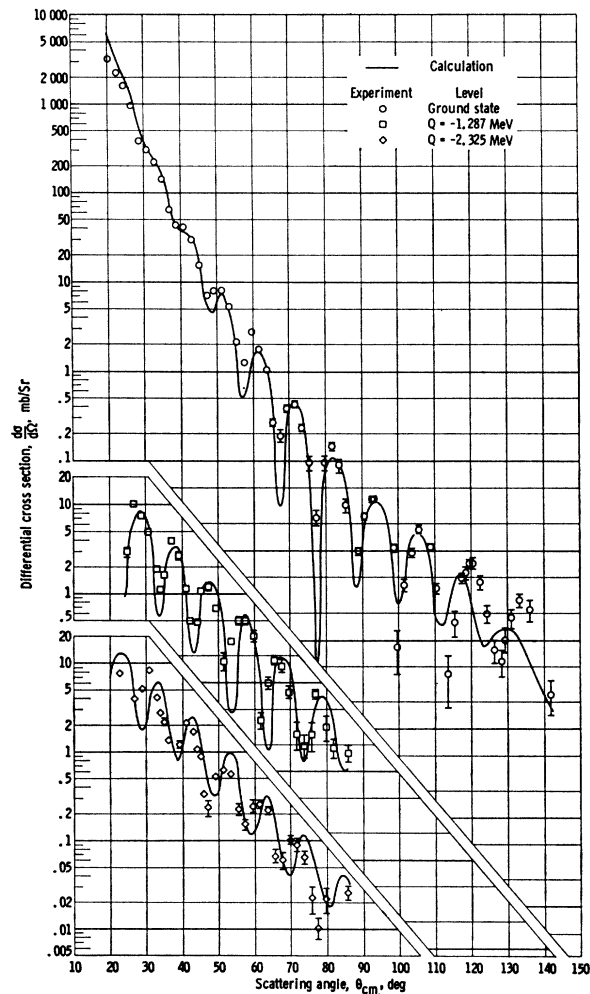


FIG. 3. Angular distributions (experimental and theoretical) for elastic and inelastic scattering of 40-MeV alpha particles from ^{116}Sn .

TABLE I. Summary of black disk and DWBA analyses of inelastic scattering.

Tin-isotope target	Excitation energy (MeV)	Spin parity J^π	Distorted-wave Born approximation deformation parameter, β_{DWBA}	Fraunhofer deformation parameter β_{Fr}	Coulomb-excitation deformation parameter, β_C
^{116}Sn	1.287	2^+	0.13 ± 0.04	0.11	0.11
	2.325	3^-	0.15 ± 0.03
^{118}Sn	1.207	2^+	0.10 ± 0.02	...	0.12
	2.359	3^-	0.15 ± 0.03
^{120}Sn	1.176	2^+	0.12 ± 0.02	0.12	0.11
	2.410	3^-	0.14 ± 0.03
^{122}Sn	1.123	2^+	0.13 ± 0.03	0.10	0.11
	2.454	3^-	0.14 ± 0.03	...	0.326

and W are the depths of the real and imaginary parts, respectively, of the nuclear optical potential, and A is the mass number of the target nucleus. In the calculation, the parameters V , W , r_0 , and a are varied in order to minimize χ^2 . In practice, it was found that attempts to optimize all four parameters simultaneously resulted in incomplete searches. Best fits were finally

obtained by fixing r_0 and searching for optimum values of the other three parameters. Repeating this procedure for various fixed values of r_0 allowed the determination of a complete set of four parameters, which minimized χ^2 .

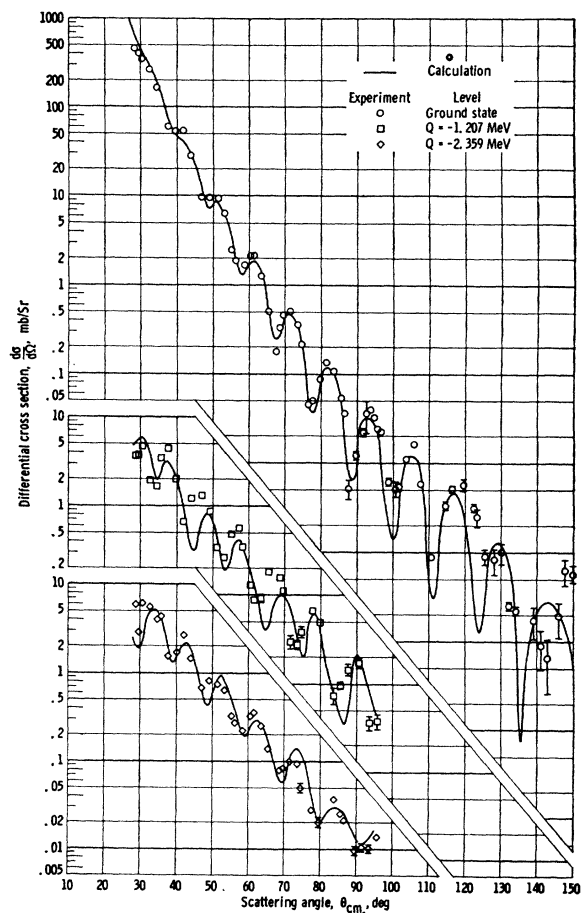


FIG. 4. Angular distributions (experimental and theoretical) for elastic and inelastic scattering of 40-MeV alpha particles from ^{118}Sn .

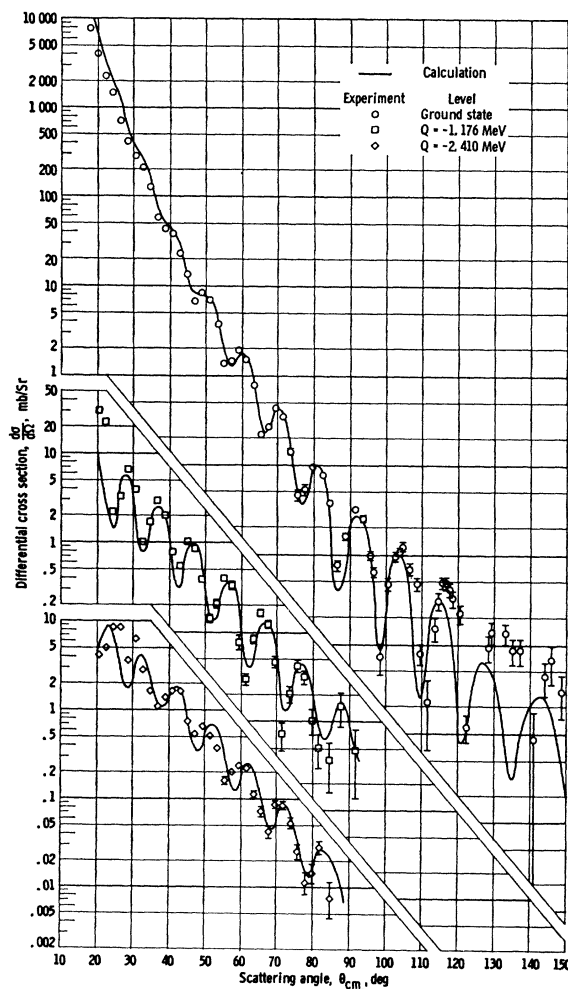


FIG. 5. Angular distributions (experimental and theoretical) for elastic and inelastic scattering of 40-MeV alpha particles from ^{120}Sn .

TABLE II. Summary of black-disk and optical-model analysis of elastic scattering.

Tin-isotope target	Strength of real part of nuclear optical potential V (MeV)	Strength of imaginary part of nuclear optical parameter W (MeV)	Diffuseness parameter a (F)	Nuclear radius constant r_0 (F)	Total reaction cross section (mb)	Optical model radius R_{OM} (F)	Fraunhofer radius R_{Fr} (F)
^{116}Sn	60.1	18.7	0.712	1.46	1888	7.83	7.88
^{118}Sn	61.8	26.3	0.671	1.46	1896	7.83	7.82
^{120}Sn	58.0	28.0	0.708	1.46	1981	7.91	7.98
^{122}Sn	62.1	30.3	0.684	1.46	1991	7.91	8.02

The optical-model parameters that gave the best fit to the data are listed in Table II along with the calculated total cross sections, which are in good agreement with the values measured by Wilkins.⁵ The angular distributions predicted by these optical potentials are compared with the experimental data in Figs. 3 to 6. There were many other sets of optical-model param-

eters, however, which were found to give almost equally satisfactory fits to the experimental data. Several sets of parameters which fit the ^{120}Sn data almost as well as those in Table II are listed with relative values of χ^2 in Table III.

All the satisfactory potentials were found to be identical beyond a radius of about $8F$, indicating that elastic scattering occurs mainly at the nuclear surface. This effect was first noticed by Igo⁶ in an analysis of data on elastic alpha scattering from argon, copper, and lead. The size of the nuclear radius given by the application of Blair's sharp-cutoff model⁷ is listed in Table II as R_{Fr} and is indeed seen to be about $8F$. A similar value for the nuclear radius is readily obtained from optical-model parameters when we define

$$R_{OM} \equiv r_0 A^{1/3} + a.$$

These values are also listed in Table II.

ANALYSIS OF INELASTIC-SCATTERING DATA

Blair Sharp-Cutoff Analysis

Attempts to determine the deformation parameters for the 2^+ states by normalizing to the Fraunhofer prediction⁷ for the most forward experimental peak were satisfactory only for ^{116}Sn , ^{120}Sn , and ^{122}Sn , since the data for ^{118}Sn were not carried far enough forward to give a suitable peak for normalizing. These Fraunhofer deformation parameters β_{Fr} are listed in Table I.

Distorted-Wave Born Approximation Analysis

The cross section in the distorted-wave approximation is

$$\frac{d\sigma}{d\Omega} = \left(\frac{2m}{4\pi\hbar^2}\right)^2 \frac{k'}{k} \sum_{\text{final states}} |\langle \psi_{k'} | K | \psi_k \rangle|^2 \quad (2)$$

where K is the transition form factor. In the collective-vibrational model the form factor for transition from the ground state of an even nucleus to an excited one-

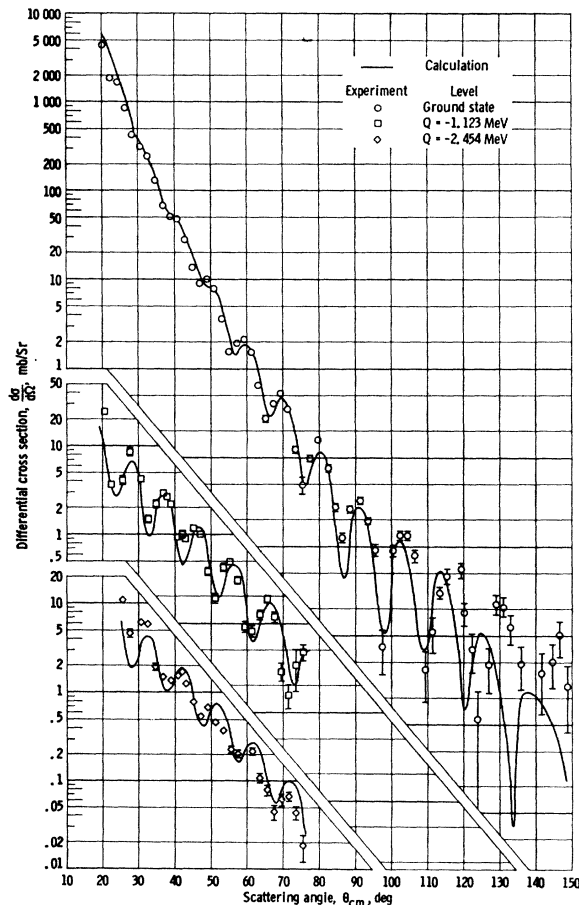


FIG. 6. Angular distributions (experimental and theoretical) for elastic and inelastic scattering of 40-MeV alpha particles from ^{122}Sn .

⁵ G. Igo and B. D. Wilkins, Phys. Rev. **131**, 1251 (1963).

⁶ G. Igo, Phys. Rev. **115**, 1665 (1959).

⁷ J. S. Blair, Phys. Rev. **115**, 928 (1959).

TABLE III. Alternative optical-model parameters for ^{120}Sn .

Strength of real part of nuclear optical potential V (MeV)	Strength of imaginary part of nuclear optical potential W (MeV)	Diffuseness parameter a (F)	Nuclear radius constant r_0 (F)	χ^2 ratio to best fit for ^{120}Sn (parameters listed in Table I)
316	145.0	0.710	1.19	4.00
117	48.0	0.707	1.36	1.04
103	42.6	0.705	1.38	1.03
87.7	38.5	0.708	1.40	1.02
66.1	31.1	0.710	1.44	1.00
52.0	24.9	0.703	1.48	1.02
43.4	22.5	0.710	1.50	1.02

phonon state of angular momentum L is

$$K(\mathbf{r}) = Y_L^M(\hat{r}) (\beta_J r_0 A^{1/3}) (2J+1)^{-1/2} (d/dr) U(\mathbf{r}), \quad (3)$$

where U is the optical potential, and $r_0 A^{1/3}$ is the nuclear radius. The parameter β_J , which is a measure of the vibrational amplitude, is determined by normalizing the calculated differential cross section to the experimental data. All other parameters are determined from fitting the elastic scattering data with the optical model. The DWBA is not capable of accounting for two-step processes, which are important in excitation of two-phonon states,^{8,9} so the calculations made are based on the assumption that these strong excitations are one-phonon states. The optical parameters are those listed in Table II. Angular distributions, calculated with the D.R.C. code¹⁰ using Eq. (3) are shown in Figs. 3 to 6 along with the experimental data for both 2^+ and 3^- states. The deformation parameters determined from the normalization are listed in Table I.

The excitation of collective states can also be studied using a particle model.^{1,11,12} The form factor consists of a constructively coherent sum of single particle terms, which in the pairing plus $Q \cdot Q$ or $O \cdot O$ interaction model¹ is given by the expression

$$K(\mathbf{r}) = i^L Y_L^M(\hat{r}) \frac{\frac{1}{2} N_L}{(2L+1)^{1/2}} \sum_{jj'} \langle j' || i^L Y_L || j \rangle^2 U_{j'j}^2 \times \frac{E_j + E_{j'}}{(E_j + E_{j'})^2 - (\hbar\omega)^2} \int dr' r'^2 R_{j'}(r') w_L(r') R_j(r') \times \int dr' r'^2 R_{j'}(r') v_L(r, r') R_j(r'), \quad (4)$$

⁸ B. Buck, Phys. Rev. **130**, 712 (1963), Phys. Rev. **127**, 940 (1962).

⁹ J. G. Wills, Ph.D. thesis, University of Washington, 1963, (unpublished).

¹⁰ W. R. Gibbs, V. A. Madsen, J. A. Miller, W. Tobocman, E. C. Cox, and L. Mowry, National Aeronautics and Space Administration Report No. NASA TN D-2170, 1963 (unpublished).

¹¹ L. S. Kisslinger, Phys. Rev. **129**, 1316 (1963).

¹² S. Yoshida, Nucl. Phys. **38**, 380 (1962), Phys. Rev. **123**, 2122 (1961).

where N_L is a normalization constant, $U_{j'j}$ is the combination of occupation parameters $U_j V_{j'} + V_j U_{j'}$, E_j is the j -level quasiparticle energy, w_L is the radial part of the single-particle multipole operator, and $v_L(r, r')$ is the radial harmonic of the alpha-nucleon interaction.

A comparison of calculations using the particle-model form factor with the experimental data is shown in Figs. 7 to 10. The optical parameters used in these calculations were $r_0 = 1.46$ F, $V = 60.5$ MeV, $W = 25$ MeV, and $a = 0.693$ F for all isotopes, so the ratios of absolute cross sections given by the calculations will depend only on differences in the wave functions and not on differences in optical parameters. This procedure is justified by the quality of the optical-model fits to the elastic-scattering data using the uniform set of parameters. A comparison for ^{116}Sn is shown in Fig. 11. The alpha-

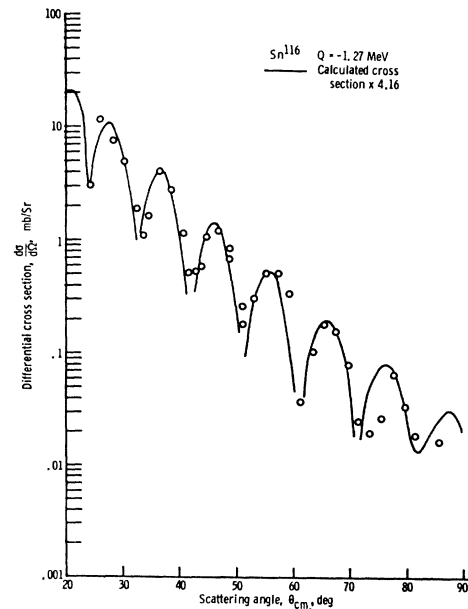


Fig. 7. Comparison with experiment of the $^{116}\text{Sn}(\alpha, \alpha')$ differential cross section calculated using particle-model nuclear wave functions (calculated cross section multiplied by 4.16).

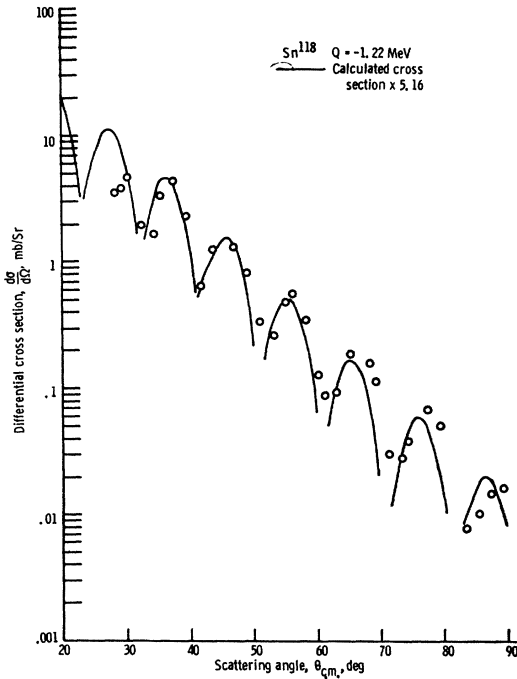


FIG. 8. Comparison with experiment of the ^{118}Sn (α, α') differential cross section calculated using particle-model nuclear wave functions (calculated cross section multiplied by 5.16).

nucleon interaction was taken to be a linear combination of two Yukawa form factors with a strength appropriate to the Gammel-Thaler² 40-MeV phenomenological potential. The calculations were made using only the nuclear cloud¹² configurations, those neutron levels in the major shell beyond neutron and proton magic numbers of 50. [The coefficients of the radial integrals in Eq. (4) were taken from Yoshida's work.¹²] The binding-well parameters are standard nucleon-optical parameters $r_0=1.25$ and $a=0.65$. The well depth is determined from the single-particle binding energy, which for all isotopes is taken to be 7.5 MeV for the $3s_{1/2}$ level. Energies relative to it were taken from Kisslinger and Sorensen's paper.¹³ As was previously found,¹ the absolute magnitudes are not highly sensitive to small changes in the binding energies.

The calculated cross sections shown in Figs. 7 to 10 are low by a factor of approximately 4. This discrepancy can be understood in the following way. Yoshida¹² has treated forward-angle scattering by using the adiabatic approximation.⁷ He finds that the cross section for multipole transition of order λ is proportional to the quantity $S_\lambda^2(\hbar\omega_\lambda)/S_\lambda'(\hbar\omega)$ where

$$S_\lambda = \sum_{ij'} \frac{E_{j'} + E_j}{(E_{j'} + E_j)^2 - (\hbar\omega_\lambda)^2} \langle j' || i^\lambda Y_\lambda w_\lambda || j \rangle^2 U_{j'j}^2 \quad (5)$$

¹³ L. S. Kisslinger and R. A. Sorensen, Rev. Mod. Phys. 35, 853 (1963).

and S_λ' is its derivative with respect to $\hbar\omega$. The quantity S_λ has the same coherence properties as the form factor Eq. (4), so Yoshida's results and the cross section calculated from Eq. (4) should be closely related. Yoshida has tabulated quantities $S_2^{(1)}$ and $S_2'^{(1)}$, which are limited to nuclear cloud configurations, as well as S_2 and S_2' which include all configurations. Since the cross section calculated herein includes only cloud configurations, we may obtain an estimate of the error incurred by calculating the cross-section ratio expected from Yoshida's result using the adiabatic approximation with only cloud configurations to that including all configurations,

$$\left\{ \frac{[S_2^{(1)}(\hbar\omega)]^2}{S_2'^{(1)}(\hbar\omega)} \right\} \left\{ \frac{[S_2(\hbar\omega)]^2}{S_2'(\hbar\omega)} \right\}^{-1} \quad (6)$$

This ratio turns out to be about 0.17, which is not greatly different from the ratio that we have obtained of about 0.25 of calculated to experimental cross section.

Aside from the question of absolute magnitude, it is interesting to compare the calculated cross-section ratios with the experimental values. It is expected that the cloud configurations alone will give a good representation of these ratios since the extracloud configurations give nearly the same fractional contribution to S_2 and S_2' for all the even tin isotopes. The calculated and experimental ratios of cross section to average cross section for all isotopes are listed in Tables IV and V. It

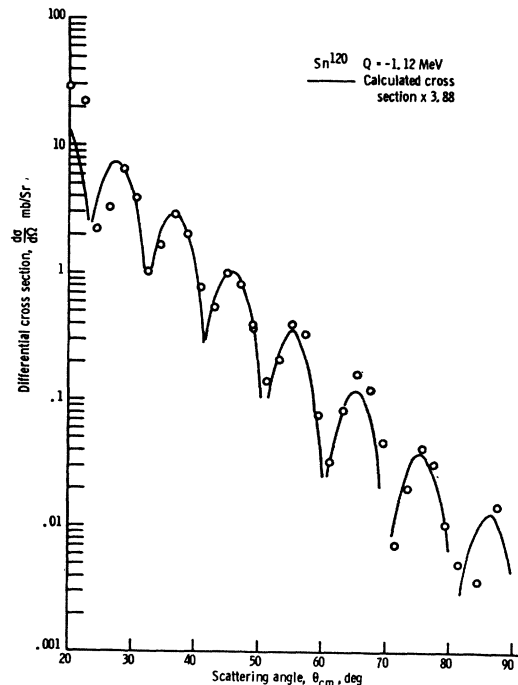


FIG. 9. Comparison with experiment of the ^{120}Sn (α, α') differential cross section calculated using particle-model nuclear wave functions (calculated cross section multiplied by 3.88).

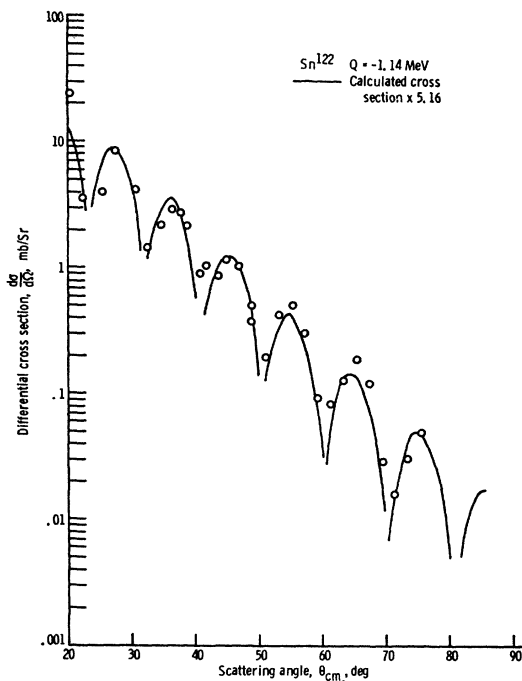


FIG. 10. Comparison with experiment of the ^{122}Sn (α, α') differential cross section calculated using particle-model nuclear wave functions (calculated cross section multiplied by 5.16).

is seen that the calculated ratios show a monotonic decrease with mass number. The experimental values also tend to decrease with mass number, but the decrease is somewhat erratic. The calculated ratios were tested to see if variation of the binding energies of the single-particle levels with separation energy from isotope to isotope would improve the agreement. This change affected the results only slightly.

DISCUSSION AND CONCLUSION

In Figs. 3 to 6 it may be observed that the experimental angular distributions of the first excited state (2^+) are out phase with the elastic distribution, while those of the second excited state (3^-) are in phase with the elastic distribution. Hence, the Blair phase rule is obeyed. In addition, the magnitudes of the 3^- cross sections are only slightly smaller than the 2^+ cross sections, which by comparison with the experimental

TABLE IV. Ratio of absolute cross section to average.^a

Atomic mass number, A	Experimental ratio	Calculated ratio ^b (uniform)	Calculated ratio ^c (best)
116	1.14	1.19	1.22
118	1.23	1.07	1.20
120	0.81	0.90	0.80
122	0.82	0.83	0.76

^a Obtained using the absolute differential cross section at the 37° peak. The average is over the four isotopes of tin, A-116, 118, 120, 122.

^b Calculated using uniform optical parameters quoted in the text.

^c Calculated using best-fit optical parameters listed in Table II.

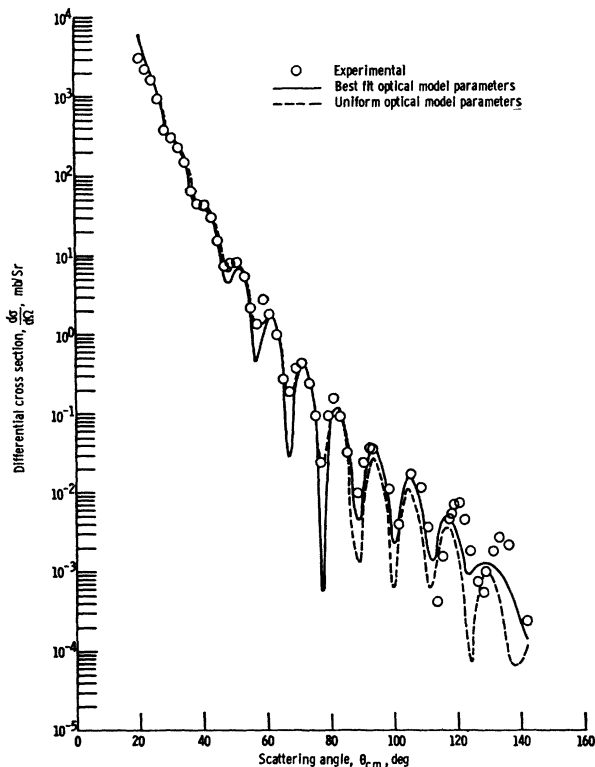


FIG. 11. Comparison of optical model fits with uniform optical parameters, $r_0 = 1.46$ F, $V = 60.5$ MeV, $W = 25$ MeV, $a = 0.693$ F with best-fit optical parameters listed in Table II for the isotope ^{116}Sn .

results of Saudinos¹⁴ for 44-MeV alpha particle scattering in the iron-nickel region would rule out the possibility that they are 4^+ two-phonon states.

The optical model analysis provides a potential which is typical of those usually obtained from analysis of elastic alpha scattering. The potential, however, is not unique and others can be found which fit the experimental data very nearly as well. The similarity of the outer edges of good potentials and the results of the sharp-cutoff analysis are consistent with the concept that alpha-particle scattering is a surface phenomenon with more deeply penetrating particles being absorbed.⁶

TABLE V. Ratio of total cross section to average.

A	Experimental ratio ^a	Calculated ratio
116	1.12	1.23
118	1.21	1.08
120	0.81	0.95
122	0.86	0.76

^a The experimental total cross sections were computed by multiplying the calculated total cross sections by the factors quoted in Figs. 7-10 needed to bring the calculated cross sections into agreement with experiment.

¹⁴ R. Beurtey, P. Catillon, R. Chaminade, M. Crut, H. Faraggi, A. Papineau, J. Saudinos, and J. Thirion, *Compt. Rend.* **252**, 1756 (1961); and J. Saudinos, France, Commissariat à l'Énergie Atomique Rept. No. 2146, 1962 (unpublished).

The DWBA calculations using the vibrational model fit the experimental angular distributions quite well. If the spins had not already been known they could have been assigned on the basis of the vibrational model, since calculations based on other spin assignments differ considerably at forward angles. Values of the nuclear-deformation parameter β_J obtained using the vibrational model are shown in Table I. Also shown in Table I are: (a) deformation parameters β_2 measured by Stelson and McGowan¹⁵ using Coulomb excitation, and (b) one β_3 value obtained using the Bohr-Mottelson formula, from the $B(E3)$ values of Hansen and Nathan,¹⁶ who measured the angular correlation of gamma rays in coincidence with back-scattered 18.5-MeV alpha particles. The agreement between values of β_2 measured by the two methods is satisfactory. The β_3 values determined here, however, are smaller by about a factor of 2.3 than that measured by Hansen and Nathan. McGowan *et al.*,¹⁷ who measured β_3 values for some of the same isotopes (¹¹⁰Cd, ¹¹²Cd, ¹¹⁴Cd, ¹¹⁶Cd) reported in reference 16, also found values that are smaller than Hansen and Nathan's by factors of 2 to 2.5.

The angular distributions obtained using the particle model also fit the data quite well. As in Ref. 1, there is a slight tendency for the calculated curves to peak at slightly lower angles than the experimental points. The two-Yukawa-potential approximation to the Gammel-Thaler 40-MeV phenomenological proton-alpha interaction gives a cross section which is lower than experiment by a factor of about 4. This result seems to be in rough agreement with that expected from only the cloud-nucleons' configurations on the basis of Yoshida's estimate using the adiabatic approximation. This result, along with the Yoshida's success in calculating $E2$ transition rates of the right order of magnitude,¹¹ indicates that the extent of configuration mixing given by the pairing plus $Q \cdot Q$ potential is sufficient to explain collective properties of these nuclei.

¹⁵ P. H. Stelson and F. K. McGowan, *Phys. Rev.* **110**, 489 (1958).

¹⁶ O. Hansen and O. Nathan, *Nucl. Phys.* **42**, 197 (1963).

¹⁷ F. K. McGowan, R. L. Robinson, P. H. Stelson, J. L. C. Ford, and W. T. Milner, *Bull. Am. Phys. Soc.* **9**, 107 (1964); F. K. McGowan, R. L. Robinson, P. H. Stelson, and J. L. C. Ford, Jr., *Nucl. Phys.* **66**, 97 (1965).

It was found previously¹ that good agreement with the absolute cross section could be obtained for ⁵⁸Ni (α, α') using the same alpha-nucleon interaction form factor with about 50 percent greater strength than that used here for the tin isotopes. The former strength was taken from the Gammel-Thaler analysis² of 10-MeV proton scattering from alpha particles, while the 40-MeV strength² used here is probably more appropriate. Thus, use of the 40-MeV strength for the ⁵⁸Ni (α, α') calculation would have resulted in a cross section low by only a factor of about 2, as compared with 4 in the tin isotopes. However, the nickel wave functions of Kisslinger¹¹ did include some core nucleons, the $1f_{7/2}$ shell neutrons, while those used here for tin did not include any extra-cloud nucleons. The two calculations thus appear to be roughly consistent.

The calculated cross sections (Table IV) drop off smoothly with increasing isotope number, whereas the experimental cross sections are about equal for ¹¹⁶Sn and ¹¹⁸Sn and again for ¹²⁰Sn and ¹²²Sn. Since the calculated cross sections are not sensitive to small changes from isotope to isotope of the single-particle-binding energies or to optical parameters, it is concluded that inelastic alpha scattering is a sufficiently accurate tool for testing nuclear wave functions systematically, and that in the case of tin the pairing plus $Q \cdot Q$ eigenfunctions do not describe in sufficient detail the differences between even isotopes.

ACKNOWLEDGMENTS

We are grateful to Dr. S. Yoshida of Osaka University for supplying us with the wave functions for the tin isotopes. We wish to thank Dr. Yoshida, Dr. W. Tobocman of Case Institute of Technology, and Dr. L. Schecter and Dr. C. D. Zafiratos of Oregon State University for reading the manuscript and making helpful suggestions. We also wish to thank Dr. F. Gangemi of Southern Oregon College for some help with numerical calculation and Donald Freeman of Lawrence Radiation Laboratory, Livermore, for assistance with the DRC program. Lawrence Radiation Laboratory, Livermore, kindly made available computer time for part of the calculations.